Stability Charts for 3D Failures of Steep Slopes Subjected to Seismic Excitation

Radoslaw L. Michalowski, F.ASCE[1]; and Tabetha Martel, S.M.ASCE[2]

Abstract: Design of slopes and analysis of existing slopes subjected to seismic shaking are carried out routinely using approximations of plane strain and substitution of a quasi-static load for the seismic excitation. A three-dimensional (3D) analysis of slopes is carried out, based on the kinematic theorem of limit analysis. A rotational failure mechanism is used with the failure surface in the shape of a curvilinear cone sector passing through the slope toe, typical of steep slopes. A quasi-static approach is used to develop stability charts allowing assessment of the factor of safety of slopes without the need for an iterative procedure. The charts are of practical importance in cases of excavation slopes and whenever a slope is physically constrained, preventing a plane failure.

DOI: 10.1061/(ASCE)GT.1943-5606.0000412

CE Database subject headings: Slope stability; Seismic effects; Limit states; Three-dimensional analysis; Failures.

Author keywords: Slopes; Stability; Seismic analysis; Limit state analysis; 3D analysis; Failure.

Introduction

The routine assumption of plane failure in slope stability analyses may be an overly conservative approach to stability assessment of slopes with a well-defined extent of the failure mechanism. This is clearly the case, for instance, in excavation slopes. An indication of this conservatism is included in the example in the latter part of this note. Recent developments in limit analysis with three-dimensional (3D) failure mechanisms (Michalowski and Drescher 2009; Michalowski 2010) make a tractable 3D analysis with seismic effects possible. The contribution in this note is in extending this 3D analysis to seismic loads and presenting the outcome in charts that do not require iterative procedures to read the safety factor. The seismic excitation is included as a quasi-static uniformly distributed horizontal load. Such an analysis, by nature, does not reflect the true influence of the seismic load with its duration, periodicity, and amplification, but it does constitute a tool allowing for a quantitative assessment of safety. The analysis is limited to steep slopes, for which the failure mechanism is expected to pass through the toe.

The 3D analyses of slope stability are often attempted using an approximate method of limit equilibrium, which requires global equilibrium (force equilibrium) of the blocks that the failing mass is divided into (for instance, Hungr 1987). As the problem is statically indeterminate, additional static, often arbitrary, assumptions are made. The second class of methods includes numerical approaches, such as the finite-element method (FEM) (for instance, Griffiths and Marquez 2007), and they allow assessment of deformation prior to failure. These methods are better suited to produce solutions for specific, well-defined slopes, rather than yield a tool for safety assessment for a wide range of parameters. Finally, the limit analysis approach can yield a rigorous bound to the safety factor. While approximate, optimization of the failure mechanism assures that the solution is a good estimate of the "true" safety factor. This was confirmed by calculations of Chen (1975), who concluded that the rotational mechanism for slopes failing under plane strain conditions is the most critical one. Similar conclusions follow from comparisons of limit analysis results and the finite element calculations (e.g., Griffiths and Lane 1999; Lane and Griffiths 1997). The kinematic approach of limit analysis is used in this note.

Limit analysis is a method that is well suited for slope stability analysis, even though the slope stability problem is not a typical problem where a boundary limit load is sought. Practical analyses call for the factor of safety, and the charts here are developed in a manner that allows for reading the safety factor without the need for iterations.

First, the limit analysis method is briefly reviewed, followed by the description of the 3D mechanism used to develop the charts. An example illustrates the use of the developed tool.

Kinematic Approach with 3D Mechanisms

Limit analysis is a well-established method for assessment of stability of structures, and the reader will find the theorems of limit analysis and their early application to slope stability problems in Drucker et al. (1952) and Drucker and Prager (1952). A variety of solutions to a wide range of problems using this method can be found in the monograph by Chen (1975).

For the theorems to be applicable, the yield surface for the soil

[1]Professor, Dept. of Civil and Environmental Engineering, Univ. of Michigan, Ann Arbor, MI 48109 (corresponding author). E-mail: rlmich@umich.edu

[2]Formerly, Graduate Research Assistant, Dept. of Civil and Environmental Engineering, Univ. of Michigan, Ann Arbor, MI 48109.

Note. This manuscript was submitted on January 17, 2010; approved on July 9, 2010; published online on January 14, 2011. Discussion period open until July 1, 2011; separate discussions must be submitted for individual papers. This technical note is part of the ***Journal of Geotechnical and Geoenvironmental Engineering***, Vol. 137, No. 2, February 1, 2011. ©ASCE, ISSN 1090-0241/2011/2-183–189/$25.00.

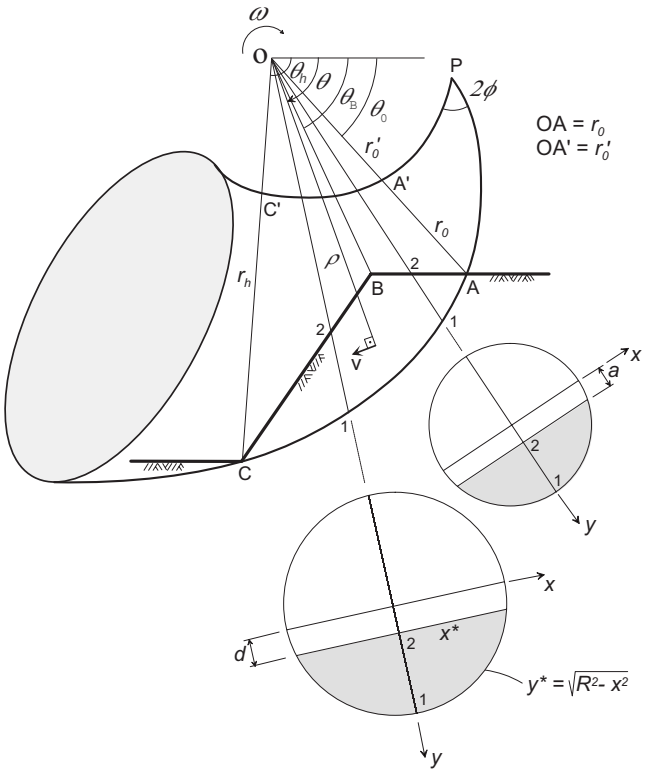

Fig. 1. Cross section of the 3D rotational failure mechanism (adapted from Michalowski and Drescher 2009)

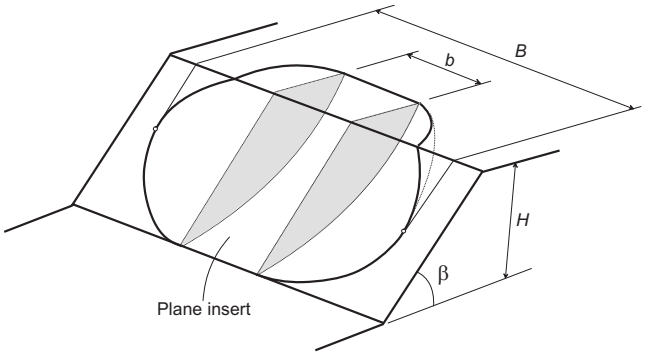

Fig. 2. 3D slope failure mechanism modified with a plane insert (adapted from Michalowski and Drescher 2009)

needs to be convex in the stress space and the deformation needs to be governed by the normality rule. There have been only a few attempts at 3D analyses using the kinematic approach of limit analysis. These include a single and multiblock translation mechanisms (Drescher 1983; Michalowski 1989), and rotational mechanisms (de Buhan and Garnier 1998; Michalowski and Drescher 2009). The 3D failures for purely cohesive soils were considered earlier by Baligh and Azzouz (1975) and Gens et al. (1988).

The kinematic approach of limit analysis is used here, and the slope problem is formulated in terms of the factor of safety. The yielding of soil is described by the Mohr-Coulomb yield condition which, for the 3D analysis, can be represented conveniently as six planes in the principal stress space

$$f(\sigma_i,\sigma_j) = \sigma_i - \sigma_j - (\sigma_i + \sigma_j)\sin\phi - 2c\cos\phi = 0; \quad i,j = 1,2,3 \tag{1}$$

where σ_i and σ_j=extremal principal stresses; ϕ=internal friction angle; and c=cohesion intercept. This yield condition reduces to a more familiar form for plane strain conditions

$$f(\sigma_x,\sigma_y,\tau_{xy}) = \sqrt{(\sigma_x - \sigma_y)^2 + 4\tau_{xy}^2} - (\sigma_x + \sigma_y)\sin\phi - 2c\cos\phi = 0 \tag{2}$$

The safety factor, F, is then defined as a ratio of the soil strength parameters to those that are necessary to reach limit equilibrium

$$F = \frac{c}{c_d} = \frac{\tan\phi}{\tan\phi_d} \tag{3}$$

where subscript d indicates the parameters "developed" at the instant of limit equilibrium. It has been pointed out (Michalowski 2010) that the kinematic approach to slopes leads to an upper bound on the safety factor so formulated.

The mechanism of failure considered here is adopted from a recent paper by Michalowski and Drescher (2009). The mechanism cross section with a vertical plane perpendicular to the crest line of the slope is shown in Fig. 1. The failing soil block is a portion of a curvilinear cone with an apex angle of 2ϕ. The failure surface is generated by a circle of increasing diameter rotated about an axis passing through point O. This shape is analogous to the surface considered earlier in a 3D translational mechanism for calculations of bearing capacity of square and rectangular footings (Michalowski 2001). The velocity within the moving block represents a rotational field and is described by

$$v = \rho\omega \tag{4}$$

where ρ=radius from point O to a point where the velocity is determined and ω=angular velocity about O. The velocities of soil particles are perpendicular to radius ρ (Fig. 1).

The contour of the surface on the central cross section is marked by two log spirals PAC

$$r = r_o e^{(\theta-\theta_o)\tan\phi} \tag{5}$$

and PA′C′

$$r' = r_o' e^{-(\theta-\theta_o)\tan\phi} \tag{6}$$

with angle θ measured as indicated in Fig. 1. Such geometry assures that the velocity of the rotating soil mass is inclined at ϕ to the failure surface at any point on the surface. The latter is necessary for the mechanism in a frictional material to be kinematically admissible. The term kinematical admissibility relates to deformation that is consistent with strain rates and velocity discontinuities predicted by the normality flow rule used in the plasticity model. The total width of the mechanism is constrained to width B.

Before performing limit analysis calculations, the mechanism in Fig. 1 was modified by adding a plane insert in the central portion of the mechanism, Fig. 2. The geometry of this insert is identical to the geometry of the plane mechanism considered by Chen et al. (1969). This assures that the combined mechanism tends to a plane mechanism when no constraints are placed on the mechanism width.

Because the surface of sliding can be viewed as being generated by a circle of radius $(r-r')/2$, the geometrical description of the surface is qualitatively different, depending on whether the generating circle is rotated about an axis outside the circle, or about its chord. This second case was also considered when de-

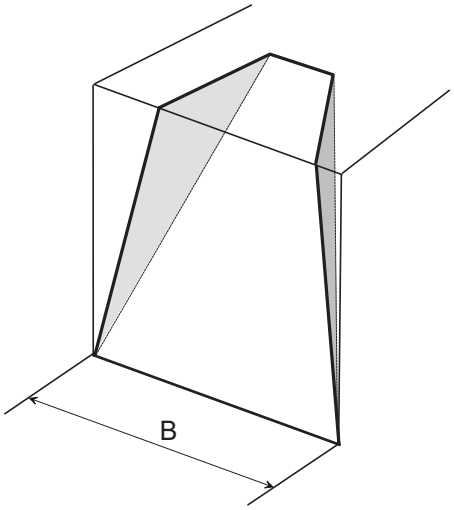

Fig. 3. One-block translational mechanism (adapted from Drescher 1983)

veloping the charts, and a more detailed description of both mechanisms can be found in Michalowski and Drescher (2009). In rare cases (vertical slopes and narrow mechanisms, $B/H=1$), a one-block translational mechanism considered earlier by Drescher (1983), Fig. 3, assured a safety factor lower than the rotational mechanism in Fig. 2.

Work Rate of Quasi-Static Seismic Force

The kinematic theorem of limit analysis indicates that an upper bound to the critical height or the factor of safety of a slope can be found from the balance of the work rate written for a kinematically admissible failure mechanism (Michalowski 2010). This balance equation contains the rate of work that is dissipated, D (internal work), and the rate of work of external forces. For a slope with traction-free boundaries, the latter includes the rate of work of the material weight, W_γ, and the work rate of the quasi-static seismic force, W_s. In general, this balance takes the form

$$D^{3D} + D^{2D} = W_\gamma^{3D} + W_\gamma^{2D} + W_s^{3D} + W_s^{2D} \tag{7}$$

where superscript 3D denotes the work rates for the 3D portion of the failure mechanism and 2D relates to the plane insert (Fig. 2).

The rate of dissipation and the rate of work of the soil weight for the 3D portion of the mechanism were described in detail in Michalowski and Drescher (2009), whereas the components for the plane insert can be found in Chen (1975). The rate of work of the quasi-static seismic force in the plane insert can be found in Chen and Liu (1990) and Michalowski and You (2000), and here we present only the term that describes the work rate of the seismic force in the 3D portion of the mechanism.

The seismic load is substituted with a distributed horizontal load, with the magnitude being fraction k_h of the soil unit weight, or

$$k_h = \frac{a_h}{g} \tag{8}$$

where a_h=horizontal ground acceleration and g=gravity acceleration. The outward seismic force is consistent with the horizontal seismic acceleration pointing into the slope. Vertical shaking is not considered directly, but it can be included with an appropriate modification of the unit weight (in such case the horizontal seismic coefficient has to be adjusted accordingly). The work rate term accounting for the rate of work of the horizontal seismic load can be written in a general form as

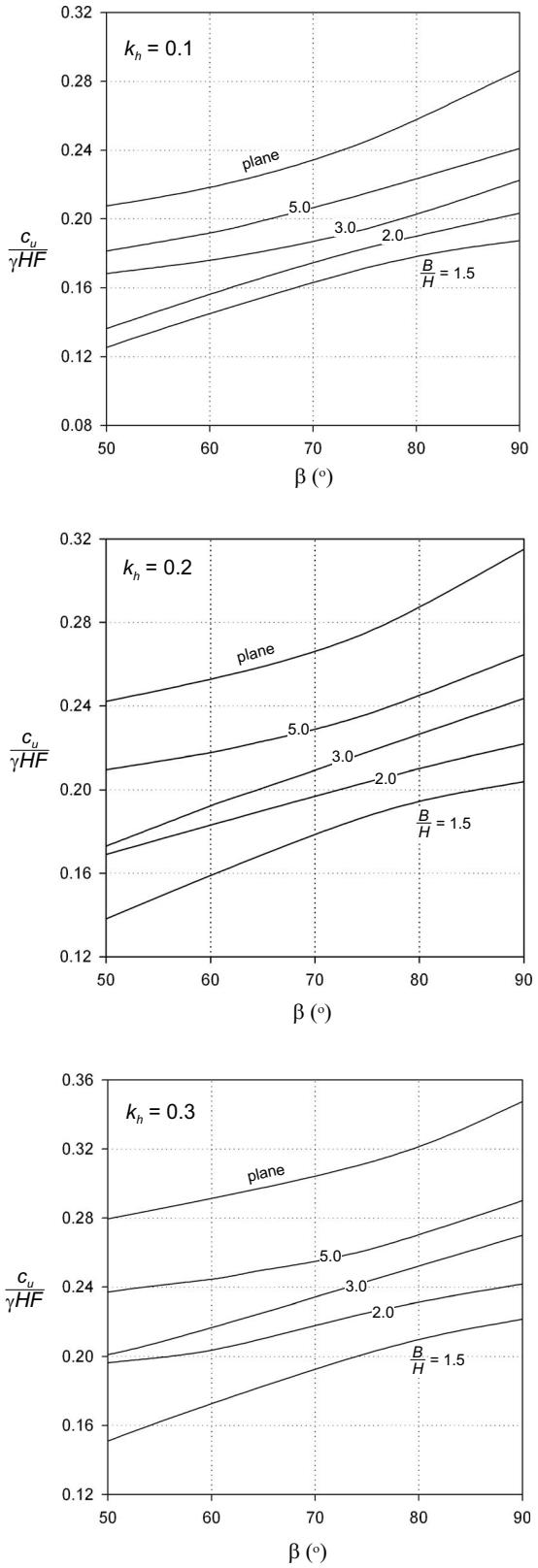

Fig. 4. Stability number for undrained slopes ($\phi=0$)

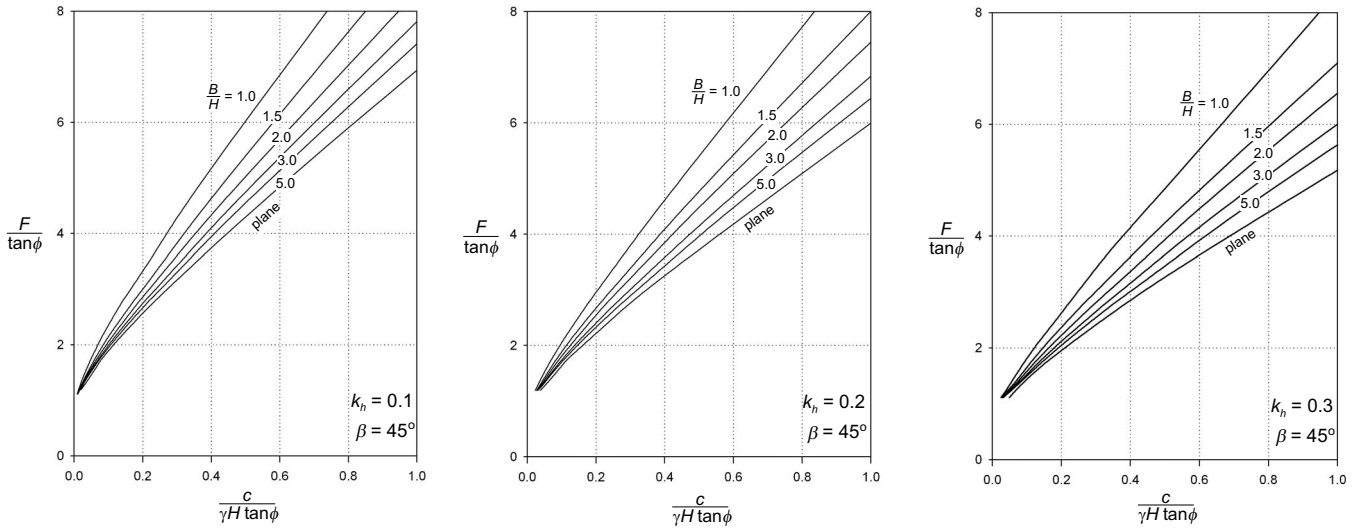

Fig. 5. Safety factor for 3D slope failure: slope inclination 45°

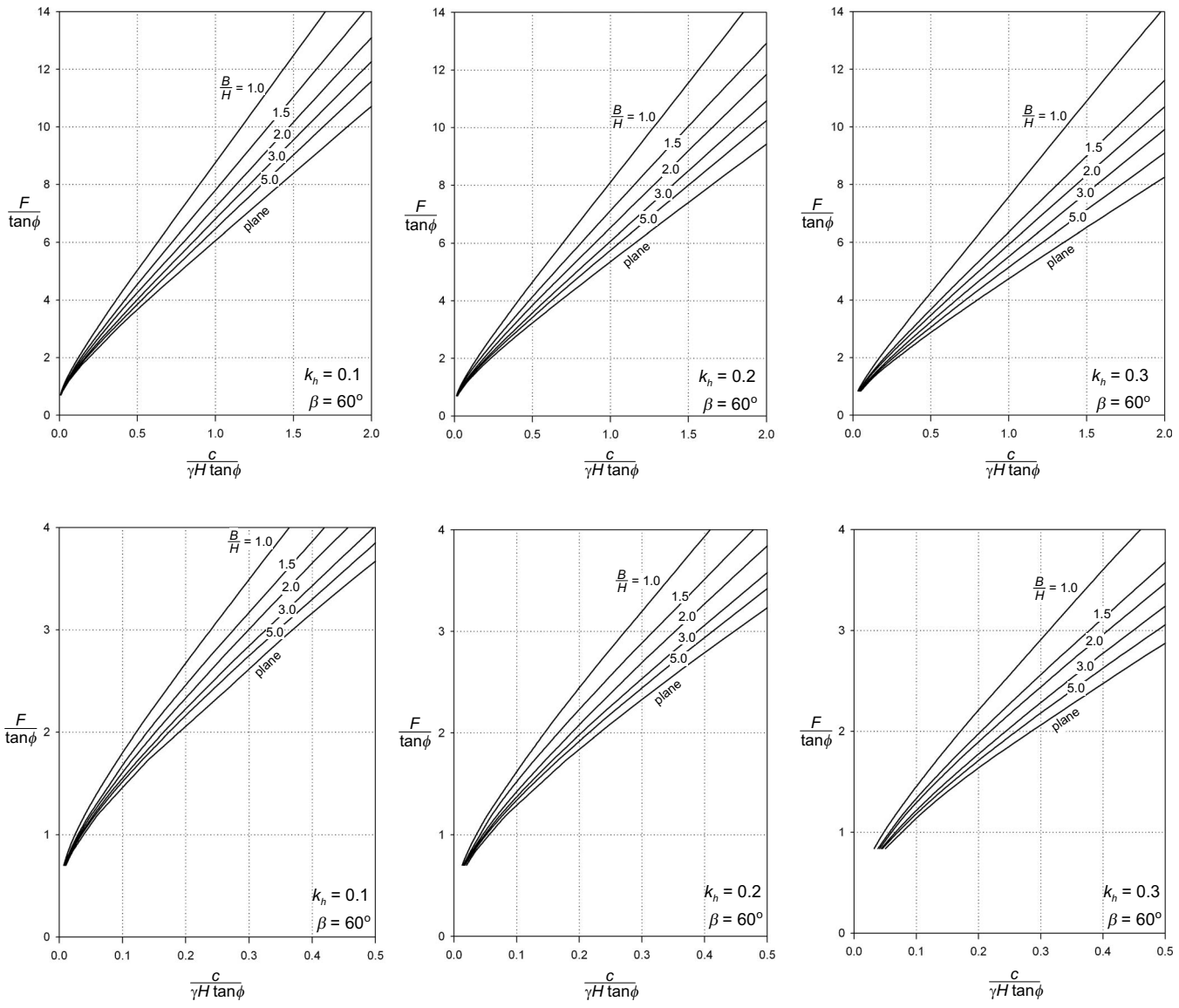

Fig. 6. Safety factor for 3D slope failure: slope inclination 60°

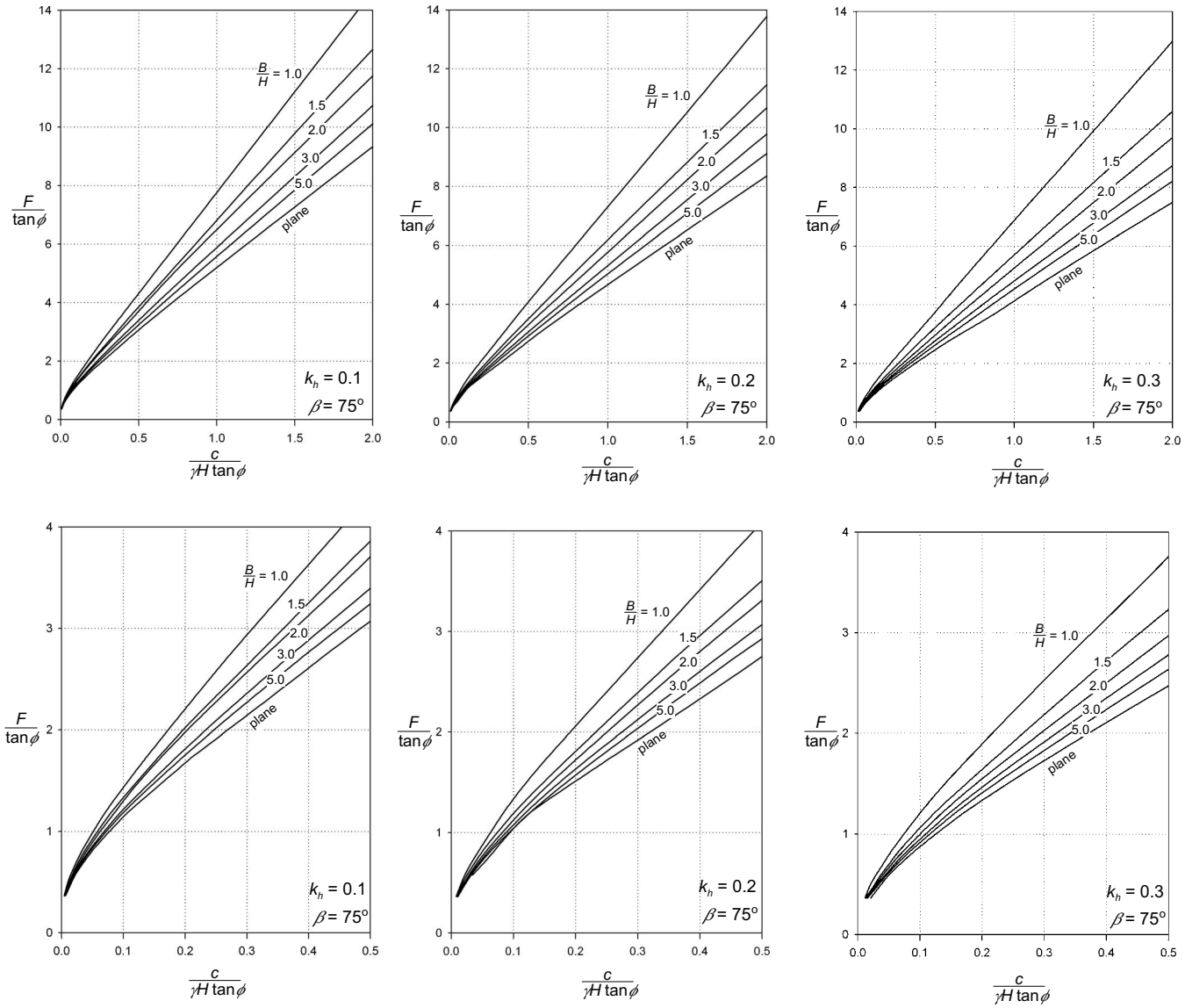

Fig. 7. Safety factor for 3D slope failure: slope inclination 75°

$$W_s^{3D} = k_h \bar{W}_s^{3D} = k_h \gamma \int_V v \sin\theta dV \tag{9}$$

where v=velocity magnitude and γ=unit weight of soil. The shape of the rotating volume V is complicated, and the details of integration are given in the Appendix.

Stability Charts

The analysis developed so far allows for calculations of safety factors in steep slopes, for which the failure mechanism is expected to pass through the toe, and for slopes with no phreatic surface present within the failure mechanism (no pore-water pressure, while matric suction enters the analysis through its influence on cohesion).

Computations were carried out for steep slopes, with inclination angles β ranging from 50° to 90° for slopes failing in undrained conditions ($\phi=0$) and between 45° and 90° for $\phi>0$. The search for the most critical mechanism was subject to a constraint on the total width of the mechanism B/H. The balance equation in Eq. (7) was transformed to calculate dimensionless critical height $\gamma H/c$, and its minimum (best upper bound) was obtained by minimizing its value with variable parameters θ_0, θ_h, r_0'/r_0, and the relative width of the plane insert b/H, subject to constraint B/H on the overall width of the mechanism. These variables are illustrated in Figs. 1 and 2.

The results of calculations are presented in Figs. 4–8. Stability number $c_u/\gamma HF$ (as defined by Taylor 1937) is illustrated in Fig. 4 for undrained slopes. The safety factor F can easily be found by reading $c_u/\gamma HF$ for a slope of given inclination and width B/H, and dividing the actual value $c_u/\gamma H$ for the slope by the read stability number. For $\phi>0$, the magnitude of $F/\tan\phi$ (or $1/\tan\phi_d$) is plotted in Figs. 5–8 as function of $c/\gamma H\tan\phi$. Such presentation allows one to avoid iteration when reading the safety factor from the charts. This is because quantity $c/\gamma H\tan\phi$ is independent of the safety factor, i.e., $c/\gamma H\tan\phi = c_d/\gamma H\tan\phi_d$. In slopes made of purely frictional soils ($c=0$), the solutions converge to shallow failures approaching the slope surface, as for plane-strain solutions. However, this is not likely to be a case for partially submerged slopes (Michalowski 2009).

All charts are presented for seismic coefficient k_h ranging from

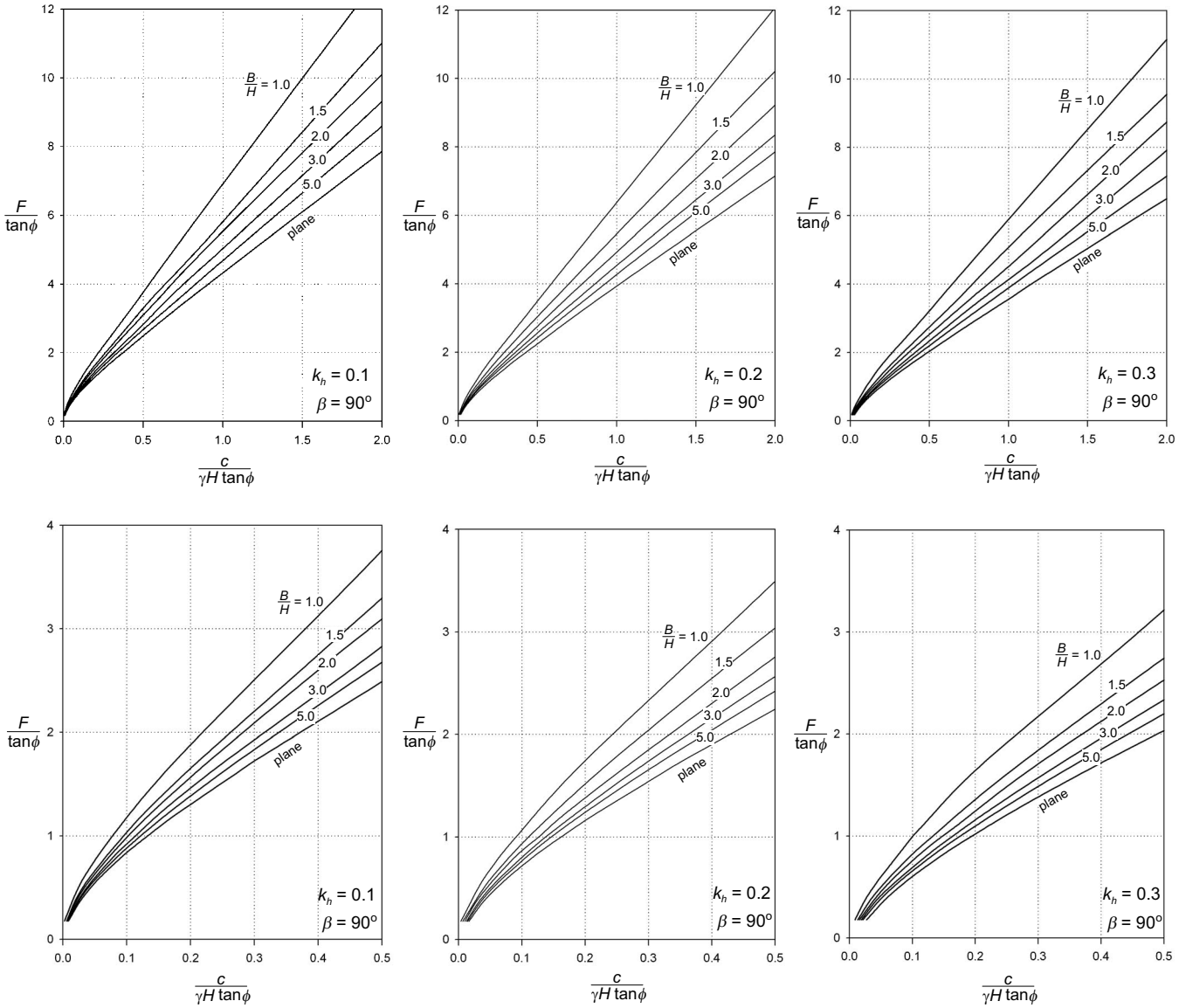

Fig. 8. Safety factor for 3D slope failure: slope inclination 90°

0.1 to 0.3. For $\phi > 0$ and $\beta \geq 60°$, two charts are presented for every combination of parameters, with the second chart focusing on a small range of variable $c/\gamma H \tan\phi$. The relative width of the mechanism of failure, B/H, ranges from 1 (1.5 for $\phi = 0$) to 5; in addition, the solution for the case of the plane mechanism is plotted (after Michalowski 2002).

It is evident that the safety factor for a slope of given inclination is dependent on the relative width of the mechanism (B/H) and the magnitude of the horizontal acceleration characterized by the fraction k_h of gravity acceleration. Only toe mechanisms were considered for 3D failures. The plane solutions, however, included both toe and under-the-toe failures, whichever lead to the minimum safety factor. However, the range of parameters for presentation of results was selected to exclude slopes for which under-the-toe failures resulted in plane strain. This is why the solutions are presented in Fig. 5 for a range of $c/\gamma H \tan\phi$ smaller than that for the steeper slopes in Figs. 6–8. The 3D failures for steep slopes are likely to be less prone to under-the-toe collapse than the two-dimensional failures, but this statement is yet to be validated with the development of a 3D limit analysis with a below-toe failure surface.

Example

A 1:1 slope has a height of 15 m, and it is built of a uniform soil characterized by $\phi = 20°$, $c = 40$ kPa, and $\gamma = 18$ kN/m^3. The extent of the slope (width) is limited by rock formations spread 30 m apart ($B/H = 2$). What would the factor of safety of this slope be if the magnitude of the horizontal acceleration were 0.2 of the gravity acceleration? First, calculate $c/\gamma H \tan\phi = 0.407$; next, read $F/\tan\phi$ from Fig. 5: $F/\tan\phi \approx 3.90$. Consequently, $F = 3.90 \cdot \tan 20° \approx 1.42$. Using plane-strain solution for this slope would yield the safety factor of about 1.18, which is quite a conservative estimate of the safety factor. The safety factor of this slope without seismic influence can be found from charts in Michalowski (2010): $F \approx 1.82$.

Final Remarks

Limit analysis is a convenient tool for considering stability of slopes. The analysis presented includes 3D and seismic effects, but it is limited to steep slopes (toe failure). Consideration of

seismic effect as a steady loading is approximate, and it does not account for the temporal effects (or periodicity) during seismic shaking. However, the charts produced are a convenient means for evaluating stability, and they do not require an iterative procedure for estimating the safety factor. Further work will concentrate on constructing a 3D mechanism applicable to shallow slopes (under-the-toe failure), and accounting for the influence of pore-water pressure on 3D stability.

Acknowledgments

The work presented in this note was carried out while both writers were supported by the National Science Foundation, Grant No. CMMI-0724022, and the senior writer was also supported by the Army Research Office, Grant No. W911NF-08-1-0376. This support is greatly appreciated.

Appendix

The contours of the curvilinear cone in Fig. 1 are described in Eqs. (5) and (6). The shape of this cone is generated by a circle of varying radius R with its center described by radius r_m

$$R = \frac{r - r'}{2}; \quad r_m = \frac{r + r'}{2} \tag{10}$$

A local coordinate system x, y in each radial cross section is now introduced, as shown in Fig. 1 (x perpendicular to the plane of the figure). The velocity in Eq. (4) during rotation about point O is now expressed as

$$v = (r_m + y)\omega \tag{11}$$

where ω=angular velocity about O. The infinitesimal volume element is

$$dV = dxdy(r_m + y)d\theta \tag{12}$$

and the work rate of the distributed seismic force in Eq. (9) now can be written as

$$W_s^{3D} = k_h \bar{W}_s^{3D} = 2\omega k_h \gamma \left[\int_{\theta_0}^{\theta_B} \int_0^{x^*} \int_a^{y^*} (r_m + y)^2 \sin\theta dy dx d\theta + \int_{\theta_B}^{\theta_h} \int_0^{x^*} \int_d^{y^*} (r_m + y)^2 \sin\theta dy dx d\theta \right] \tag{13}$$

The two integrals in Eq. (13) include the work of the seismic force in two portions of the rotating volume separated by the plane perpendicular to the plane of Fig. 1 and passing through points O and B. Angle θ_B defining this plane was found from the geometrical relations in Fig. 1

$$\theta_B = \arctan\frac{\sin\theta_0}{\cos\theta_0 - A}$$

$$A = \frac{\sin(\theta_h - \theta_0)}{\sin\theta_h} - \frac{e^{(\theta_h - \theta_0)\tan\phi}\sin\theta_h - \sin\theta_0}{\sin\theta_h \sin\beta}\sin(\theta_h + \beta) \tag{14}$$

The upper integration limit on y is a function of x: $y^* = \sqrt{R^2 - x^2}$, and the limits on x are $x^* = \sqrt{R^2 - a^2}$ and $x^* = \sqrt{R^2 - d^2}$ in the first and the second integral, respectively, and a and d are given in

$$a = \frac{\sin\theta_0}{\sin\theta} r_0 - r_m; \quad d = \frac{\sin(\beta + \theta_h)}{\sin(\beta + \theta)} r_0 e^{(\theta_h - \theta_0)\tan\phi} - r_m \tag{15}$$

The integrals in Eq. (13) were calculated analytically with respect to x and y, and integration over angle θ was carried out numerically.

References

Baligh, M. M., and Azzouz, A. S. (1975). "End effects on stability of cohesive slopes." *J. Geotech. Engrg. Div.*, 101(11), 1105–1117.

Chen, W. F. (1975). *Limit analysis and soil plasticity*, Elsevier, Rotterdam, The Netherlands.

Chen, W. F., Giger, M. W., and Fang, H. Y. (1969). "Limit analysis of stability of slopes." *Soils Found.*, 9(4), 23–32.

Chen, W. F., and Liu, X. L. (1990). *Limit analysis in soil mechanics*, Elsevier Science, Amsterdam, The Netherlands.

de Buhan, P., and Garnier, D. (1998). "Three dimensional bearing capacity analysis of a foundation near a slope." *Soils Found.*, 38(3), 153–163.

Drescher, A. (1983). "Limit plasticity approach to piping in bins." *J. Appl. Mech.*, 50, 549–553.

Drucker, D. C., and Prager, W. (1952). "Soil mechanics and plastic analysis or limit design." *Q. Appl. Math.*, 10(2), 157–165.

Drucker, D. C., Prager, W., and Greenberg, H. J. (1952). "Extended limit design theorems for continuous media." *Q. Appl. Math.*, 9, 381–389.

Gens, A., Hutchinson, J. N., and Cavounidis, S. (1988). "Three-dimensional analysis of slides in cohesive soils." *Geotechnique*, 38(1), 1–23.

Griffiths, D. V., and Lane, P. A. (1999). "Slope stability analysis by finite elements." *Geotechnique*, 49(3), 387–403.

Griffiths, D. V., and Marquez, R. M. (2007). "Three-dimensional slope stability analysis by elasto-plastic finite elements." *Geotechnique*, 57(6), 537–546.

Hungr, O. (1987). "Extension of Bishop's simplified method of slope stability analysis to three dimensions." *Geotechnique*, 37(1), 113–117.

Lane, P. A., and Griffiths, D. V. (1997). "Finite element slope stability analysis—Why are engineers still drawing circles?" *Proc., 6th Int. Symp. on Numerical Models in Geomechanics (NUMOG VI)*, Balkema, Rotterdam, The Netherlands, 589–593.

Michalowski, R. L. (1989). "Three-dimensional analysis of locally loaded slopes." *Geotechnique*, 39(1), 27–38.

Michalowski, R. L. (2001). "Upper-bound load estimates on square and rectangular footings." *Geotechnique*, 51(9), 787–798.

Michalowski, R. L. (2002). "Stability charts for uniform slopes." *J. Geotech. Geoenviron. Eng.*, 128(4), 351–355.

Michalowski, R. L. (2009). "Critical pool level and stability of slopes in granular soils." *J. Geotech. Geoenviron. Eng.*, 135(3), 444–448.

Michalowski, R. L. (2010). "Limit analysis and stability charts for 3D slope failures." *J. Geotech. Geoenviron. Eng.*, 136(4), 583–593.

Michalowski, R. L., and Drescher, A. (2009). "Three-dimensional stability of slopes and excavations." *Geotechnique*, 59(10), 839–850.

Michalowski, R. L., and You, L. (2000). "Displacement of reinforced slopes subjected to seismic loads." *J. Geotech. Geoenviron. Eng.*, 126(8), 685–694.

Taylor, D. W. (1937). "Stability of earth slopes." *J. Boston Soc. Civ. Eng.*, 24(3), 197–246, reprinted in Contributions to Soil Mechanics 1925 to 1940, Boston Society of Civil Engineers, Boston 1963, 337–386.